



Research article

Stiffening of the gluteal muscle increased the intramuscular stress: An in-silico implication of deep tissue injury

Jingyi Jia^{a,b}, Shengbo Gong^{a,b}, Aili Zhang^a, Liping Jiang^c, Yifei Yao^{a,b,*}^a School of Biomedical Engineering, Med-X Research Institute, Shanghai Jiao Tong University, 1954 Huashan Road, Shanghai 200030, China^b Engineering Research Center of Digital Medicine and Clinical Translation, Ministry of Education, 1954 Huashan Road, Shanghai Jiao Tong University, Shanghai 200030, China^c Nursing Department, Xinhua Hospital Affiliated to Shanghai Jiao Tong University School of Medicine, 1665 Kongjiang Road, Shanghai 200092, China

ARTICLE INFO

Keywords:

Deep tissue injury
Muscle spasm
Muscle shear modulus
Finite element analysis
Intramuscular stress

ABSTRACT

Objectives: Deep tissue injury is a common form of pressure ulcers in muscle tissues under bony prominences caused by sustained pressure or shear, which has a great impact on patients with restricted mobility such as spinal cord injury. Frequent spasms in spinal cord injury patients featured by muscle stiffening may be one of the factors leading to deep tissue injury. The purpose of this study was to investigate the relationship between the gluteal muscle shear modulus and intramuscular compressive/shear stress/strain.

Methods: A semi-3D finite element model of the human buttock was established using COMSOL software and the acquired biomechanical data were analyzed through Pearson correlation and Spearman correlation.

Results: Results showed that the compressive stress, strain energy density, and average von Mises stress increased with the increase of the gluteal muscle shear modulus.

Conclusion: These results may indicate muscle stiffening caused by muscle spasms could lead to higher deep tissue injury development risk as well as shed light on effective treatments for relieving muscular sclerosis mechanically.

1. Introduction

Deep tissue injury (DTI) is the most severe type of pressure ulcers (PU) for its crypticity and fatality, which often occurs in muscle tissues over bony prominences caused by intensive or prolonged mechanical loading [1]. The incidence rate of DTI is increasing in the United States [2], with the proportion of 33.6% among the PU patients in 2020 [3]. DTI patients are often prone to complications, typically diabetes mellitus and spinal cord injury (SCI) [4,5]. SCI patients are extremely susceptible to PU, since PU appeared in SCI patients for approximately 33% over one year, and 90% over a lifetime [6,7].

The increased risk factors for PU in SCI patients include immobility, muscle atrophy, and spasm [8]. Spasticity is a common complication of SCI patients [9], with an incidence rate of 65%–78% in recruited chronic SCI patients for more than one year after injury [10]. In patients with spasms, friction between the body and the bed cushion can cause PU [8]. In the cellular level, spastic

* Corresponding author. School of Biomedical Engineering, Med-X Research Institute, Shanghai Jiao Tong University, 1954 Huashan Road, Shanghai 200030, China.

E-mail address: yifeiyao@sjtu.edu.cn (Y. Yao).

<https://doi.org/10.1016/j.heliyon.2023.e13459>

Received 19 November 2022; Received in revised form 27 January 2023; Accepted 31 January 2023

Available online 3 February 2023

2405-8440/© 2023 The Authors. Published by Elsevier Ltd. This is an open access article under the CC BY-NC-ND license (<http://creativecommons.org/licenses/by-nc-nd/4.0/>).

muscle cells are significantly shorter in morphology and stiffer in mechanical properties than normal cells [11]. The tangent moduli of muscle cells with spasticity were higher than the healthy ones, indicating that the change of muscle moduli was affected by spasms [11]. In the tissue level, muscle spasticity was mainly manifested as increased muscle tone and rapid muscle contractions [12]. Muscle contractions along with spasticity might lead to an abnormal increase in muscle stiffness.

Direct mechanical loading on muscle tissues has been recognized as the most important contributing factor to DTI formation [1], which can be estimated by compressive stress [13], compressive strain [1], shear stress [14], shear strain [15], strain energy density [16], or von Mises stress. However, it is difficult to measure these mechanical parameters in the clinic but can be calculated through finite element (FE) analysis. For instance, the FE model of the human buttock was established to quantify sub-dermal loads [17] or stress/strain [18] for DTI patients and healthy subjects based on the morphological data with Open MRI of specific human subjects in a seated posture. Furthermore, DTI developing risk can be quantified by incorporating damage threshold curves from in vitro [1]/vivo [19] experiments. The diffusion effect of harmful chemicals was combined with the FE model with the mechanical damage threshold curve to demonstrate metabolites causing cell damage could accelerate the propagation of the damaged area [20,21].

It is difficult to determine the material properties of muscle and fat tissues, and parameters in the literature varied due to different experimental conditions [22–25]. Inverse finite element analysis (inverse FEA) was conducted as an approach to assess the material properties [26]. “Inverse” refers to the determination of input parameters by output results, which is achieved by iteratively changing the input parameters to match the accurate experimental results [26]. In this paper, the material properties of the muscle and fat tissues in the reference model were estimated through inverse FEA with in vivo buttock contact pressure distribution.

This study aimed to investigate the relationship between the shear modulus and the intramuscular stress/strain, strain energy density, and von Mises stress of the gluteal muscle in SCI patients through a hyperelastic FE model of the human buttock. We hypothesized that there was a positive correlation between the muscle shear modulus and intramuscular stress/strain, as well as strain energy density.

2. Methods

2.1. FE modeling

A semi-3D FE cross-sectional model containing the ischial tuberosity, the muscle (gluteal muscle), the fat (fat and skin were considered as the part of fat), and the cushion was developed using COMSOL Multiphysics to simulate the stress/strain distribution in muscle tissues [21,27,28]. The process of finite element modeling was shown in Fig. 1a–d. The dimensions in x, y, and z direction were 128 mm, 100 mm and 4 mm respectively.

The mechanical properties (Table 1 [23],) of the ischial tuberosity and the cushion were considered isotropic, homogeneous, and

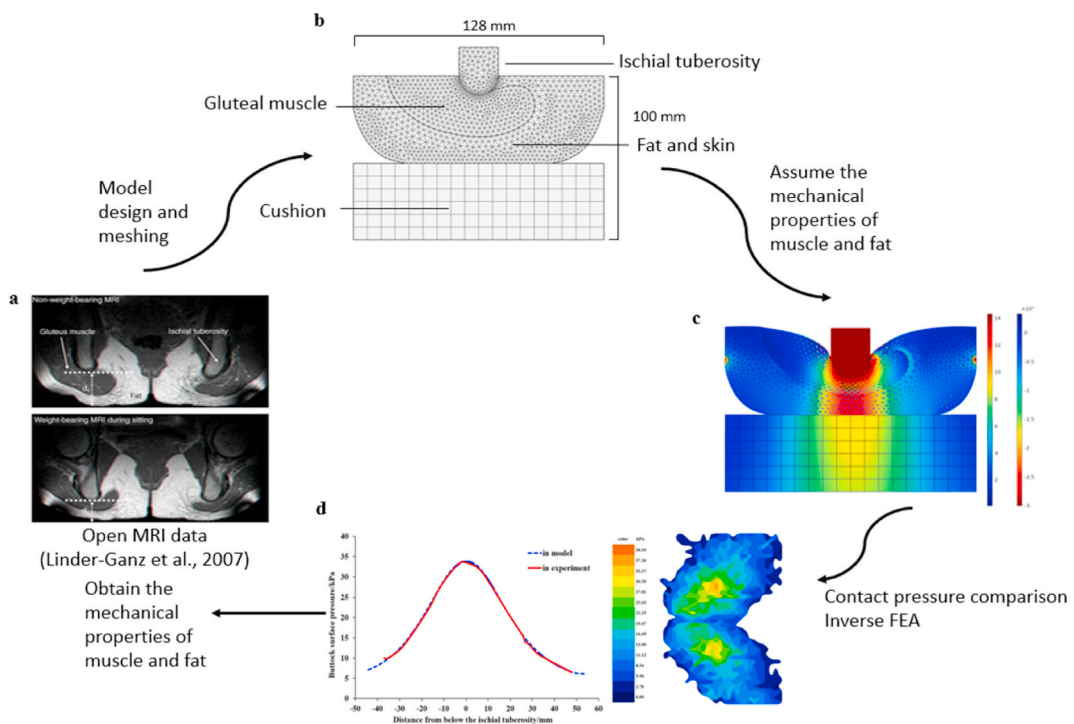


Fig. 1. Process of finite element modeling of the human buttock and cushion. (a) The open MRI data during seating; (b) the semi-3D FE model and meshing; (c) the contact pressure calculated in the FE model was compared with the (d) contact pressure obtained through the experiment.

elastic [23]. However, the material properties of the muscle and fat were set as hyperelastic and nearly incompressible with Poisson’s ratio ν as 0.49. As the stress or strain distribution in the FE model during prolonged sitting posture was considered at equilibrium status, G of muscle or fat was defined as the long-term shear modulus, which was determined using inverse FEA described in 2.2. Volume modulus κ was determined with the equation described using Eq. (1) [21].

$$\nu = \frac{3(\kappa/G) - 2}{6(\kappa/G) + 2} \tag{1}$$

We used the Ogden material model in Eq. (2) and Eq. (3) with an energy function to represent hyperelastic incompressible material behavior of muscle and fat [14,29].

$$W = \frac{\mu}{\alpha} (\lambda_1^\alpha + \lambda_2^\alpha + \lambda_3^\alpha - 3) \tag{2}$$

$$\mu = \frac{2G}{\alpha} \tag{3}$$

where λ_i ($i = 1, 2, 3$) were the principal stretch ratios, and G was the shear modulus. α of the muscle and fat were assumed as 15.7 and 3.5 respectively [22,25].

The ischial tuberosity, the muscle, and the fat were meshed with tetrahedral elements, while the cushion was meshed with hexahedral elements. A mesh convergence test was conducted to assess the optimal mesh refinement size. The mesh density corresponding to total node number 4302 was reasonable when the average compressive stress (minimum principal stress) in the muscle was taken as the key outcome parameter for mesh refinement. The errors were 0.42% and 0.52% when the mesh density was halved (node number 2285) and doubled (node number 9940). A contact pair was assigned to the interface between the buttock and the cushion by introducing a penalty factor of 2 MPa m^{-1} . The interfaces between the muscle and fat, between the muscle and ischial tuberosity, and between the fat and ischial tuberosity were defined as “tie”, constraining any relative movement between the two surfaces of the interface. The nodes of the inferior surface of the cushion were fixed in 6° of freedom. Translational boundary condition being free in-plane and fixed out-of-plane was applied at both the anterior and posterior surfaces of all the parts. The loading was estimated as 52 kPa considering the normal torso weight (650 N), which was applied to the upper surface of the ischial tuberosity in the model.

2.2. Inverse FEA and model validation

The experimental data on the contact pressure distribution of the human buttock was acquired through the body pressure measurement system (BPMS™, Tekscan, South Boston, MA). One male subject (height of 1.72 m, weight of 70 kg) sat on the BPMS pressure sensor mat until the sitting posture was steady (Fig. 2a). The sampling rate was 10 Hz with a sensing area of 42 × 48 cm² and a resolution of 1 cm × 1 cm (Fig. 2b). This study was approved by the Research Ethics Committee of Xin Hua Hospital Affiliated to Shanghai Jiao Tong University School of Medicine, and the written informed consent was obtained from the subject before participation. The contact pressure of the buttock was then analyzed to make a comparison with the contact pressure simulated in the reference model.

The assessment of the shear moduli (G) of muscle and fat was conducted in the reference model using inverse FEA. In this study, the contact pressure distribution on the interface between the buttock and the cushion in the reference model could be compared with the contact pressure distribution obtained by the BPMS pressure mat through the least-square method. The simulation of the reference model was conducted under the assumption of different shear moduli of muscle and fat within the range (100 Pa–1 MPa) obtained from literature [21–23,25,30] and keeping other parameters as constants. The shear moduli of muscle and fat were determined by inverse FEA were 239.1 Pa and 10.6 kPa in the reference model (Table 2).

2.3. Parametric analysis

Parametric analysis was conducted to evaluate the relationship between the muscle shear modulus and parameters presenting intramuscular stress/strain. The parameters measuring intramuscular stress/strain were 12 indexes including average/maximum compressive stress (absolute value of minimum principal stress), average/maximum compressive strain (absolute value of minimum principal strain), average/maximum shear stress (absolute value of shear stress tensor component on the xy -plane, σ_{xy}), average/maximum shear strain (absolute value of shear strain tensor component on the xy -plane, ϵ_{xy}), average/maximum strain energy density, and average/maximum von Mises stress. The gluteal muscle shear modulus was set as 59.75 Pa, 239.1 Pa, 295.7 Pa, 352.3 Pa, 408.9 Pa, and 465.5 Pa, where 59.75 Pa was used to simulate muscle softening, and 465.5 Pa was used to simulate muscle stiffening.

Table 1
Material properties of elastic ischial tuberosity and cushion.

Parts	E_0 (MPa)	Poisson’s	Number of elements	References of material properties
Ischial tuberosity	1000	0.3	1942	Brosh et al. (2000) [23]
Cushion	3	0.3	108	

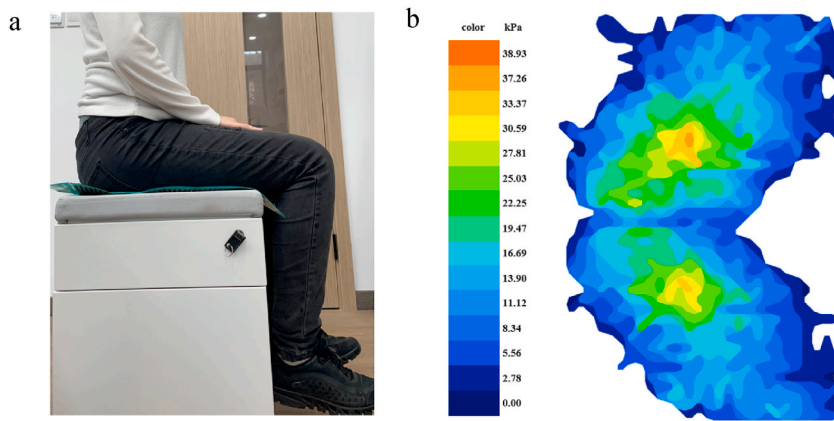


Fig. 2. The experimental setup of (a) the pressure measurement process of the subject and (b) the nephogram of contact pressure distribution of the human buttock.

Table 2
Material properties of hyperelastic muscle, fat and skin.

Parts	G (Pa)	Poisson's ratio	α	κ (kPa)	Number of elements
Muscle	239.1	0.49	15.7	11.88	5857
Fat and skin	10,600	0.49	3.5	526.82	8064

2.4. Data analysis

Pressure-time cell death threshold curve $\sigma(t)$ described the relationship between tissue mechanical strength and loading duration, shown in Eq. (4):

$$\sigma(t) = \frac{K}{1 + e^{a(t-t_0)}} + C \tag{4}$$

where K was 23 kPa, a was in the scope of 0.15 min^{-1} to 1 min^{-1} , t_0 was 90 min, and C was 9 kPa [19]. Muscle compressive stress damage threshold in this study can be estimated as approximately equaling to pressure-time cell death threshold. The percentage of the damaged area could be calculated under the $\sigma(t)$ where a was equaling to 0.15 min^{-1} to establish the percentage of damaged area-loading duration curve.

Pearson correlation analysis was used when data followed the normal distribution and determined by Kolmogorov-Smirnov normality test, showing the relationship between the gluteal muscle shear modulus and the average/maximum compressive stress, maximum strain energy density, and average von Mises stress. Furthermore, the average/maximum contact pressure at the interface between the buttock and the cushion and the average/maximum compressive stress of the gluteal muscle was also analyzed through Pearson correlation. Spearman correlation analysis was incorporated when data did not follow the normal distribution, showing the relationship between the gluteal muscle shear modulus and average strain energy density, maximum von Mises stress, average shear

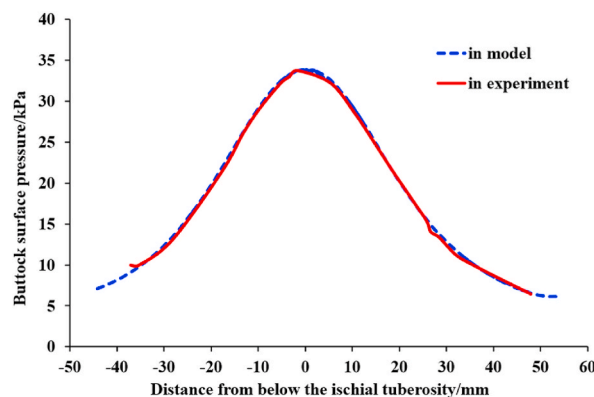


Fig. 3. FE model validation through inverse FEA.

stress, maximum shear stress, average compressive strain, maximum compressive strain, average shear strain, maximum shear strain. A p-value lower than 0.05 was considered statistically significant.

3. Results

3.1. Model validation

The geometry of the reference FE model was adjusted in accordance with the human buttock size in the experiment. The contact pressure distribution curve along the medial-lateral direction obtained in the FE model matched the curve obtained from the in vivo experiment with an error of 2.07% (Fig. 3). The displacement of the ischial tuberosity under the applied loading in the model was 14.1 mm, which was in the range of reasonable in-vivo ischial displacement (10 mm–15 mm²⁸).

3.2. Parametric analysis

Parametric analysis of the gluteal muscle shear modulus on compressive stress showed that the average/maximum compressive stresses increased with the increase of muscle shear modulus; and for shear stress, the maximum shear stress increased, but the average shear stress remained with little change (Fig. 4a and b). In contrast to the stress, the average/maximum compressive and shear strains decreased with the increase of muscle shear modulus (Fig. 4c and d). Similar to compressive stress, the average/ maximum strain energy density increased with the increase of the muscle shear modulus (Fig. 4e). The average von Mises stress decreased, but the maximum von Mises stress showed no obvious decreasing tendency, with the increase of the muscle shear modulus (Fig. 4f).

3.3. The percentage of the damaged area

The relationship between the percentage of the damaged area and the loading duration in the model followed a sigmoidal curve, with the percentage of damaged area sharply increased when the loading duration reached 60 min (Fig. 5).

Table 3 enumerated the relationship between the percentage of the damaged area and the muscle shear modulus in the long term

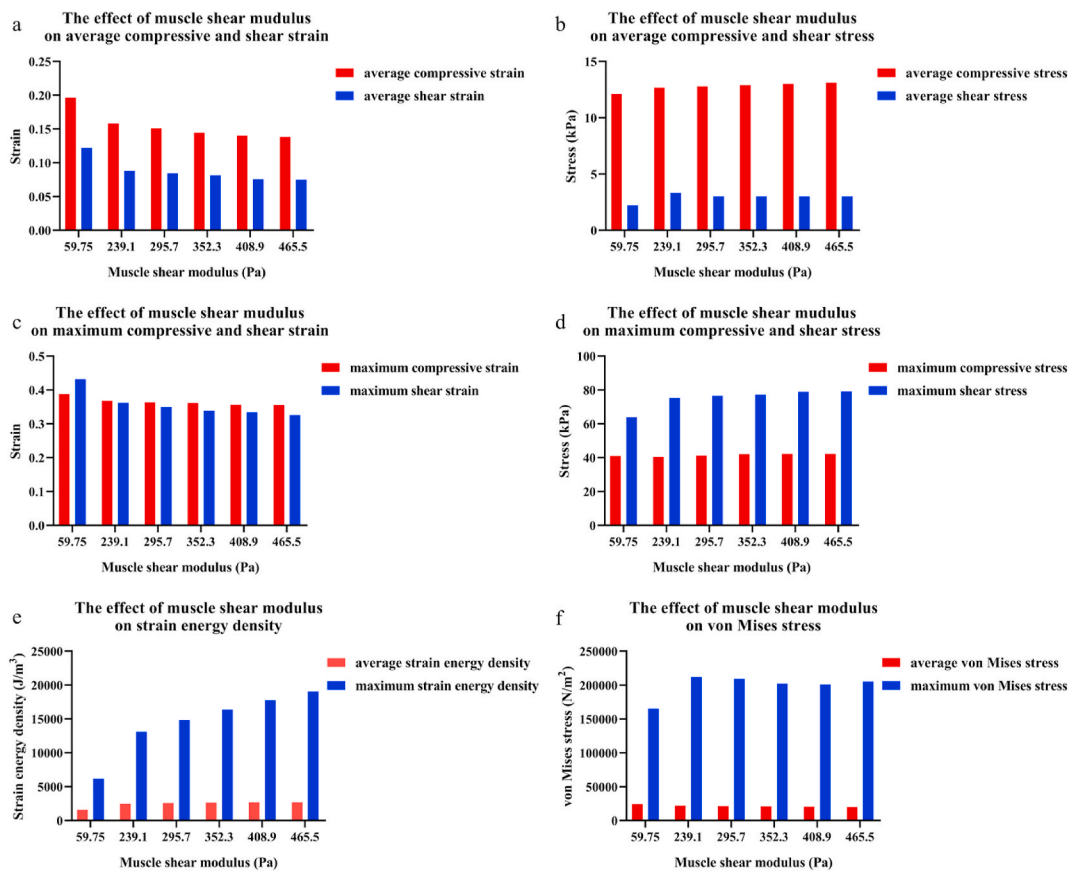


Fig. 4. Parametric analysis of (a, b) average/ maximum compressive/shear stress; (c, d) average/ maximum compressive/shear strain; (e) average/ maximum strain energy density; (f) average/ maximum von Mises stress.

(after 120 min). The percentage of the damaged area increased along with muscle shear modulus. However, as muscle shear modulus increased, the increment of the percentage of the damaged area became smaller. The percentage of the damaged area increased by 13.98% when comparing the minimum and maximum muscle shear modulus.

3.4. Correlation analysis

The results of Pearson correlation analyses indicated that average compressive stress, maximum compressive stress, and maximum strain energy density were positively correlated with the muscle shear modulus, and the correlation coefficient R-squared were 0.983 ($P < 0.002$, Fig. 6a), 0.5939 ($P = 0.073$, Figs. 6b), and 0.9858 ($P < 0.001$, Fig. 6c) respectively. The average von Mises stress was negatively correlated with the muscle shear modulus, and the correlation coefficient R-squared was 0.9862 ($P < 0.001$, Fig. 6d).

Furthermore, the average compressive stress was positively correlated with the average contact pressure, and the correlation coefficient R-squared was 0.6195 ($P < 0.001$, Fig. 7a). Similarly, the maximum compressive stress was positively correlated with the maximum contact pressure, and the correlation coefficient R-squared was 0.7078 ($P < 0.001$, Fig. 7b).

In Table 4, spearman correlation analyses showed that there was a strong positive correlation between the average strain energy density/maximum shear stress and the muscle shear modulus. The average/maximum compressive strain and average/maximum shear strain were negatively correlated with the muscle shear modulus. Furthermore, the maximum von Mises stress and average shear stress were not significantly correlated with the muscle shear modulus.

4. Discussion

This study developed a semi-3D FE model of the human buttock to analyze the relationship between muscle shear modulus and intramuscular stress/strain through inverse FEA. The results of this study showed that stiffer muscles might lead to a lower percentage of the damaged area in the short term (within 60 min) but higher damage in the long term (after 120 min). Parametric analysis further indicated that the compressive stress and strain energy density might be key parameters indicating deep tissue damage. This study suggested that DTI development risk could be decreased by adjusting the posture of SCI patients every 90 min, which was close to the suggestion from Agency for Health Care Policy and Research [31].

Parametric analysis results indicated that the changing trend of stress along with muscle stiffness was opposite to that of strain, especially the compressive stress and the compressive strain. Several studies investigated tissue damage from both stress and strain perspectives. Gefen et al. concluded that the compressive strain/stress increased with the increase of muscle stiffness [32,33]. From the conclusion of Loerakker et al. [14], the stiffer the muscle, the lower the internal shear strain/stress, which was different from our results. This might be due to the different considerations between in-plane shear stress in Loerakker et al. [14] and stress tensor in this study. This study considered shear stress/strain tensor in the xy-plane (which was the interface between ischial tuberosity and muscle) because the tissue damage might mainly be due to the shear on this interface. This contradiction could be settled by introducing strain energy density to consider the combination of the stress and strain parameters [28]. The results of strain energy density analysis showed a similar trend to that of compressive stress.

The results of Pearson correlation and Spearman correlation analyses showed that the average/maximum compressive stress and average/maximum strain energy density were positively correlated with muscle shear modulus. Thus, we suggested that the compressive stress and strain energy density might be key parameters indicating deep tissue damage. Four parameters of the strain were negatively correlated with the muscle shear modulus since the muscle deformation became smaller with the increase of muscle shear modulus under constant loading on the ischial tuberosity. As for shear stress, the maximum shear stress was positively correlated with the muscle shear modulus, but the average shear stress showed no correlation with the muscle shear modulus. This might be due to the maximum shear stress confined in a small area of muscle leading to muscle damage, which could not contribute to the overall damage in the muscle, thus there was no correlation in average shear stress. The maximum von Mises stress was not correlated with muscle shear modulus, but the average von Mises stress was negatively correlated with muscle shear modulus. This might be due to the decrease in the strain which was dominant when muscle shear modulus increased under constant loading in our FE model.

Compressive stress was proved to be one of the main parameters demonstrating tissue damage in literature, determining tissue damage by quantifying the compressive stress threshold [34,35]. As for strain and strain energy density, K.K. Ceelen et al. [16]

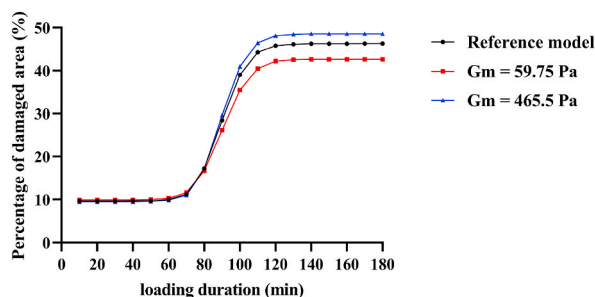


Fig. 5. The percentage of damaged area-loading duration curve under muscle shear moduli of 239.1 Pa (reference model), 59.75 Pa, and 465.5 Pa.

Table 3

The effect of muscle shear modulus on the percentage of the damaged area in the long term.

Muscle shear modulus/Pa	59.75	239.1 (Reference model)	295.7	352.3	408.9	465.5
Long-term percentage of the damaged area	42.62%	46.25%	46.91%	47.56%	48.13%	48.58%

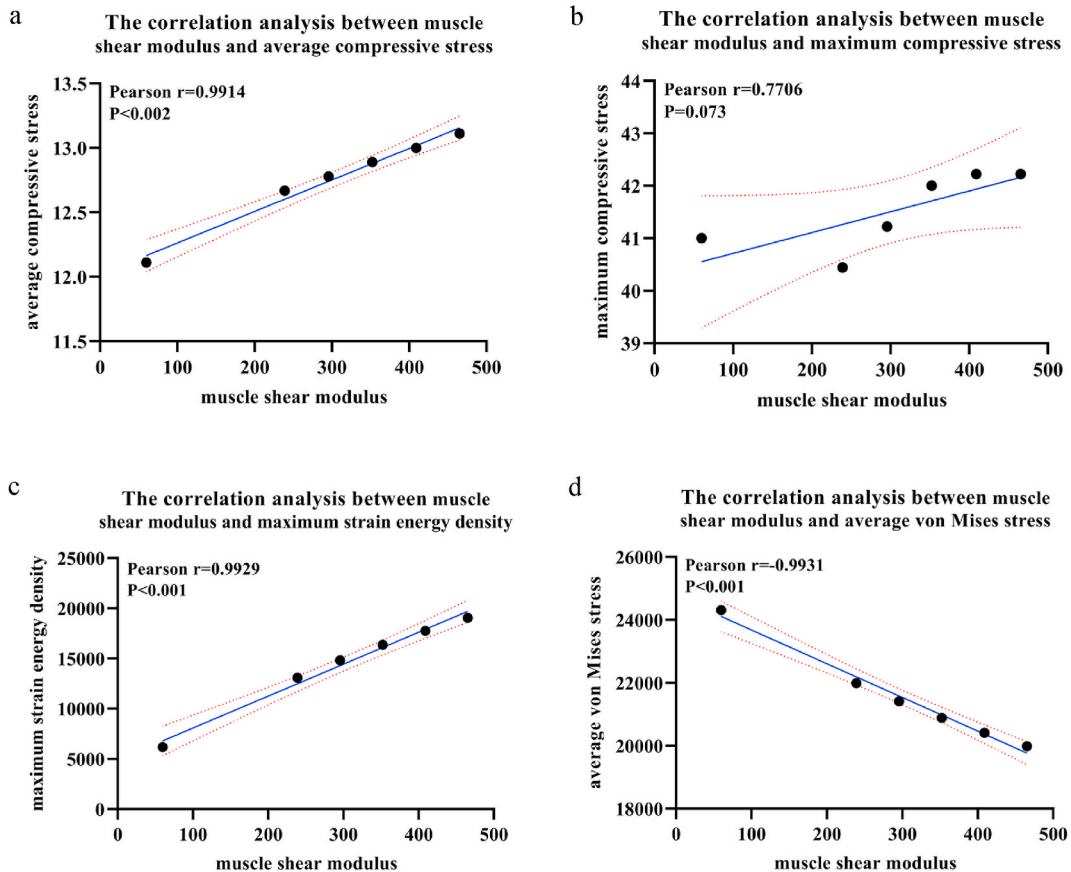


Fig. 6. Pearson correlation analysis between muscle shear modulus and (a) average compressive stress; (b) maximum compressive stress; (c) maximum strain energy density; (d) average von Mises stress. The 0.95-confidence limits were depicted as dashed lines.

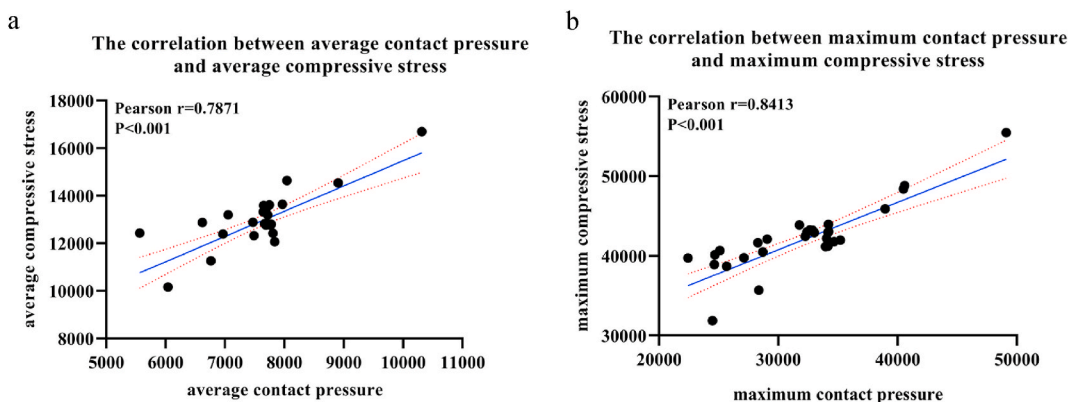


Fig. 7. Pearson correlation analysis between (a) average contact pressure at the interface between the buttock and the cushion and average compressive stress; (b) maximum contact pressure at the interface between the buttock and the cushion and maximum compressive stress. The 0.95-confidence limits were depicted as dashed lines.

Table 4
Spearman correlation analysis of intramuscular stress/strain.

Spearman Correlation	average strain energy density	maximum von Mises stress	average shear stress	maximum shear stress	average compressive strain	maximum compressive strain	average shear strain	maximum shear strain
<i>Spearman r</i>	1	0.02857	0.169	1	-1	-1	-1	-1
<i>P (two-tailed)</i>	0.003	>0.999	>0.999	0.003	0.003	0.003	0.003	0.003

examined the relationship between internal tissue strains and damage due to sustained deformation in rat muscle tissues by calculating strains through the FE model and assessing tissue damage through T2-weighted MRI [16]. Maximum shear strain, maximum compressive strain, and strain energy were taken into consideration and the results showed that the relative damaged area increased when these three parameters exceeded certain thresholds [16]. As for von Mises stress, it was considered as a parameter varying with the backrest inclination and the weight of subjects rather than material property in previous study [33]. Also, it is difficult to obtain the parameters of the von Mises stress in clinical situations. The parameter of von Mises stress might not be suggested as the key parameter indicating tissue damage.

Other studies focused on the changes in the properties of soft tissues to investigate DTI development risk, such as fat thickness, muscle atrophy, and body mass index. Wang et al. [36] analyzed the influence of subcutaneous fat thickness on the interface pressure and load distribution of the buttock through a 3D FE model, which demonstrated that the fat tissue in the buttock could reduce the contact pressure when sitting on a rigid seat. The results of Chen et al. [37] demonstrated that body mass index was the most important factor affecting the risk of buttock DTI. These studies provide support for inter-individual factors influencing DTI during sitting. However, our study mainly focused on the change of muscle stiffness of one single subject to reveal the relationship between muscle spasms and DTI development risk in SCI patients, as well as provided important mechanical parameters (compressive stress and strain energy density) indicating DTI development risk, which could further help develop clinical diagnostic methods of DTI.

Muscle spasms could be relieved by muscular relaxants or electrical stimulation, which could be further utilized to prevent DTI. For muscular relaxants, Tizanidine has been shown to reduce muscle tone and frequency of muscle spasms in SCI patients [10]. For electrical stimulation, functional electrical stimulation (FES) was useful for alleviating muscle spasms and improving muscle activity in horses [38]. Also, FES (1 h a day, 5 days a week, for 24 weeks) could partly reverse the loss of muscle strength in SCI patients [39].

Massage on muscle is a traditional approach to relieve spasms and decrease stiffness by conducting hand movements on the skin [40]. There were several theories regarding the therapeutic effects of massage, including neurological, physiological, and mechanistic (rearrangement of muscle fibers) mechanisms [41–43]. Despite individuals' perception of variance in tissue characteristics, there was no evidence indicating that soft tissue massage led to a change in the passive mechanical properties of the calf muscles [44]. Due to the diversity of the techniques and the subjects, the usefulness of massage remained difficult to prove.

To reduce the risk of DTI from environmental mechanical conditions, an appropriate cushion might be helpful. Results of an early study evaluating the effect of traditional cushions on reducing the incidence of pressure ulcers based on the contact pressure between the buttock and the cushion showed that there was no significant difference in the incidence of PU (including DTI) between subjects who continued to use cushions and those who did not [45]. The inefficiency of the cushion could be explained by lacking evidence of a correlation between external body interface pressure and intramuscular stress/strain [46]. Thus, the understanding of the relationship between contact pressure and intramuscular stress/strain is important. This study concluded that there was a strong correlation between contact pressure and intramuscular compressive stress. It is necessary to obtain an accurate prediction of intramuscular stress/strain to avoid muscle damage by adjusting the external contact pressure on the cushion. The intramuscular stress/strain could be simulated based on the mechanical properties of muscles determined through musculoskeletal imaging of elastography, especially shear-wave elasticity imaging [47].

There were several limitations in this study. First, the result from semi-3D FE model might not be the same with the simulation of the actual anatomical structure and pressure distribution from a 3D perspective. Second, the mechanical property of muscle was roughly estimated by the inverse FEA in this study, it could be more accurate to measure the muscle shear modulus by musculoskeletal elastography in the future. Third, changes in muscle geometry and shape during muscle spasms were not considered in the model, further improvements could be made by introducing in vivo tests to obtain muscle geometry variance information.

Declarations

Author contribution statement

Jingyi Jia and Shengbo Gong: Performed the experiments; Analyzed and interpreted the data; Wrote the paper. Aili Zhang and Liping Jiang: Contributed reagents, materials, analysis tools or data. Yifei Yao: Conceived and designed the experiments; Wrote the paper.

Data availability statement

Data will be made available on request.

Declaration of interest's statement

The authors declare no conflict of interests.

Additional information

No additional information is available for this paper.

Acknowledgement

The authors acknowledged the support from Shanghai Pujiang Program [19PJ1406400], National Natural Science Foundation of China [32201067], Medicine–Engineering Joint Foundation at Shanghai Jiao Tong University [YG2019ZDB02 & YG2021QN142].

References

- [1] A. Gefen, B. van Nierop, D.L. Bader, C.W.J. Oomens, Strain-time cell-death threshold for skeletal muscle in a tissue-engineered model system for deep tissue injury, *J. Biomech.* 41 (9) (2008) 2003–2012.
- [2] R. Sullivan, A two-year retrospective review of suspected deep tissue injury evolution in adult acute care patients, *Ostomy/Wound Manag.* 59 (9) (2013) 30–39.
- [3] J. Cox, L.E. Edsberg, K. Koloms, C.A. VanGilder, Pressure injuries in critical care patients in US hospitals: results of the International Pressure Ulcer Prevalence Survey, *J. Wound, Ostomy Cont. Nurs.* 49 (1) (2022) 21–28.
- [4] A. Levy, A. Gefen, Computer modeling studies to assess whether a prophylactic dressing reduces the risk for deep tissue injury in the heels of supine patients with diabetes, *Ostomy/Wound Manag.* 62 (4) (2016) 42–52.
- [5] L.R. Solis, E. Twist, P. Seres, R.B. Thompson, V.K. Mushahwar, Prevention of deep tissue injury through muscle contractions induced by intermittent electrical stimulation after spinal cord injury in pigs, *J. Appl. Physiol.* 114 (2) (1985) 286–296. , 2013.
- [6] S.L. Garber, D.H. Rintala, K.A. Hart, M.J. Fuhrer, Pressure ulcer risk in spinal cord injury: predictors of ulcer status over 3 years, *Arch. Phys. Med. Rehabil.* 81 (4) (2000) 465–471.
- [7] J.S. Krause, L. Broderick, Patterns of recurrent pressure ulcers after spinal cord injury: identification of risk and protective factors 5 or more years after onset, *Arch. Phys. Med. Rehabil.* 85 (8) (2004) 1257–1264.
- [8] J.M. Hoff, L.W. Bjerke, P.E. Gravem, E.M. Hagen, T. Rekand, Pressure ulcers after spinal cord injury, *Tidsskr. Nor. Laegeforen* 132 (7) (2012) 838–839.
- [9] S. Yoshizaki, K. Yokota, K. Kubota, T. Saito, M. Tanaka, D.-J. Konno, T. Maeda, Y. Matsumoto, Y. Nakashima, S. Okada, The beneficial aspects of spasticity in relation to ambulatory ability in mice with spinal cord injury, *Spinal Cord* 58 (5) (2020) 537–543.
- [10] M.M. Adams, A.L. Hicks, Spasticity after spinal cord injury, *Spinal Cord* 43 (10) (2005) 577–586.
- [11] J. Friden, R.L. Lieber, Spastic muscle cells are shorter and stiffer than normal cells, *Muscle Nerve* 27 (2) (2003) 157–164.
- [12] F. Wieters, C. Weiss Lucas, M. Gruhn, A. Buschges, G.R. Fink, M. Aswendt, *Exp. Neurol.* 335 (2021), 113491.
- [13] Y.F. Yao, A.F. Mak, Strengthening of C2C12 mouse myoblasts against compression damage by mild cyclic compressive stimulation, *J. Biomech.* 49 (16) (2016) 3956–3961.
- [14] S. Loerakker, L.R. Solis, D.L. Bader, F.P.T. Baaijens, V.K. Mushahwar, C.W.J. Oomens, How does muscle stiffness affect the internal deformations within the soft tissue layers of the buttocks under constant loading? *Comput. Methods Biomech. Biomed. Eng.* 16 (5) (2013) 520–529.
- [15] Y. Hong, Y. Yao, S. Wong, Change in viability of C2C12 myoblasts under compression, shear and oxidative challenges, *J. Biomech.* 49 (8) (2016) 1305–1310.
- [16] K.K. Ceelen, A. Stekelenburg, S. Loerakker, G.J. Strijkers, D.L. Bader, K. Nicolay, F.P. Baaijens, C.W.J. Oomens, Compression-induced damage and internal tissue strains are related, *J. Biomech.* 41 (16) (2008) 3399–3404.
- [17] E. Linder-Ganz, N. Shabshin, Y. Itzhak, Z. Yizhar, I. Siev-Ner, A. Gefen, Strains and stresses in sub-dermal tissues of the buttocks are greater in paraplegics than in healthy during sitting, *J. Biomech.* 41 (3) (2008) 567–580.
- [18] E. Linder-Ganz, N. Shabshin, Y. Itzhak, A. Gefen, Assessment of mechanical conditions in sub-dermal tissues during sitting: a combined experimental-MRI and finite element approach, *J. Biomech.* 40 (7) (2007) 1443–1454.
- [19] E. Linder-Ganz, S. Engelberg, M. Scheinowitz, A. Gefen, Pressure–time cell death threshold for albino rat skeletal muscles as related to pressure sore biomechanics, *J. Biomech.* 39 (14) (2006) 2725–2732.
- [20] Y.F. Yao, Z.T. Xiao, S.W. Wong, Y.-C. Hsu, T. Cheng, C.-C. Chang, L.M. Bian, A.F. Mak, The effects of oxidative stress on the compressive damage thresholds of C2C12 mouse myoblasts: implications for deep tissue injury, *Ann. Biomed. Eng.* 43 (2) (2015) 287–296.
- [21] Y.F. Yao, L.X. Da Ong, X.T. Li, K.L. Wan, A.F. Mak, Effects of biowastes released by mechanically damaged muscle cells on the propagation of deep tissue injury: a multiphysics study, *Ann. Biomed. Eng.* 45 (3) (2017) 761–774.
- [22] E.M. Bosboom, M.K. Hesselink, C.W.J. Oomens, C.V. Bouten, M.R. Drost, F.P. Baaijens, Passive transverse mechanical properties of skeletal muscle under in vivo compression, *J. Biomech.* 34 (10) (2001) 1365–1368.
- [23] T. Brosh, M. Arcan, Modeling the body/chair interaction—an integrative experimental–numerical approach, *Clin. Biomech.* 15 (3) (2000) 217–219.
- [24] K. Comley, N.A. Fleck, A Micromechanical model for the Young's modulus of adipose tissue, *Int. J. Solid Struct.* 47 (21) (2010) 2982–2990.
- [25] E. Omid, L. Fuetterer, S. Reza Mousavi, R.C. Armstrong, L.E. Flynn, A. Samani, Characterization and assessment of hyperelastic and elastic properties of decellularized human adipose tissues, *J. Biomech.* 47 (15) (2014) 3657–3663.
- [26] P. Wallia, A. Erdemir, Z.M. Li, Subject-specific finite element analysis of the carpal tunnel cross-sectional to examine tunnel area changes in response to carpal arch loading, *Clin. Biomech.* 42 (2017) 25–30.
- [27] E. Linder-Ganz, A. Gefen, Stress analyses coupled with damage laws to determine biomechanical risk factors for deep tissue injury during sitting, *J. Biomech. Eng.* 131 (1) (2009), 11003.
- [28] D.Z.T. Xiao, S.Y.Q. Wu, A.F. Mak, Accumulation of loading damage and unloading reperfusion injury—modeling of the propagation of deep tissue ulcers, *J. Biomech.* 47 (7) (2014) 1658–1664.
- [29] R.W. Ogden, Large deformation isotropic elasticity—on the correlation of theory and experiment for incompressible rubberlike solids, *Proc. R. Soc. London, Ser. A* 326 (1567) (1972) 565–584.
- [30] A. Chawla, S. Mukherjee, B. Karthikeyan, Characterization of human passive muscles for impact loads using genetic algorithm and inverse finite element methods, *Biomech. Model. Mechanobiol.* 8 (1) (2009) 67–76.
- [31] N. Bergstrom, M.A. Bennett, C.E. Carlson, Treatment of pressure ulcers, in: *Clinical Practice Guideline No. 15*, US Dept of Health and Human Services, Public Health Service, Rockville (MD), 1994. AHCPR. 95-0652.
- [32] A. Gefen, N. Gefen, E. Linder-Ganz, Margulies. In vivo muscle stiffening under bone compression promotes deep pressure sores, *S. S. J. Biomech. Eng.* 127 (3) (2005) 512–524.
- [33] E. Linder-Ganz, A. Gefen, Mechanical compression-induced pressure sores in rat hindlimb: muscle stiffness, histology, and computational models, *J. Appl. Physiol.* 96 (6) (2004) 2034–2049.
- [34] A.F. Khan, M.K. Macdonald, C. Streutker, C. Rowsell, J. Drake, T. Grantcharov, Defining the relationship between compressive stress and tissue trauma during laparoscopic surgery using human large intestine, *IEEE J. Transl. Eng. Health Med.* 7 (2019) 1–8.

- [35] A.F. Khan, M.K. MacDonald, C. Streutker, C. Rowsell, J. Drake, T. Grantcharov, Tissue stress from laparoscopic grasper use and bowel injury in humans: establishing intraoperative force boundaries, *BMJ Surg. Interv. Health Technol.* 3 (1) (2021), e000084.
- [36] K. Wang, Y.F. Chen, S.J. Huang, L.J. Wang, W.X. Niu, Subcutaneous fat thickness remarkably influences contact pressure and load distribution of buttock in seated posture, *J. Healthc. Eng.* (2021), 4496416.
- [37] Y.F. Chen, Y.X. Shen, K. Wang, Y. Qi, W.X. Niu, Y. Wang, Mechanical analysis of deep tissue injury during sitting in patients with spinal cord injury via parametric finite element model, *Biomech. Model. Mechanobiol.* 21 (5) (2022) 1573–1584.
- [38] B. Ravara, V. Gobbo, U. Carraro, L. Gelbmann, J. Pribyl, S. Schils, Functional electrical stimulation as a safe and effective treatment for equine epaxial muscle spasms: clinical evaluations and histochemical morphometry of mitochondria in muscle biopsies, *Eur. J. Transl. Myol.* 25 (2) (2015) 4910.
- [39] M. Belanger, R.B. Stein, G.D. Wheeler, T. Gordon, B. Leduc, Electrical stimulation: can it increase muscle strength and reverse osteopenia in spinal cord injured individuals? *Arch. Phys. Med. Rehabil.* 81 (8) (2000) 1090–1098.
- [40] G.C. Goats, Massage – the scientific basis of an ancient art: Part 1. The techniques, *Br. J. Sports Med.* 28 (3) (1994) 149–152.
- [41] T.M. Field, Massage therapy effects, *Am. Psychol.* 53 (12) (1998) 1270.
- [42] C.W. Karlson, N.A. Hamilton, M.A. Rapoff, Massage on experimental pain in healthy females: a randomized controlled trial, *J. Health Psychol.* 19 (3) (2014) 427–440.
- [43] A. Mouraux, L. Plaghki, Cortical interactions and integration of nociceptive and non-nociceptive somatosensory inputs in humans, *Neuroscience* 150 (1) (2007) 72–81.
- [44] D. Thomson, A. Gupta, J. Arundell, J. Crosbie, Deep soft-tissue massage applied to healthy calf muscle has no effect on passive mechanical properties: a randomized, single-blind, cross-over study, *BMC Sports Sci. Med. Rehabil.* 7 (1) (2015) 1–8.
- [45] S.L. Garber, L.R. Dyerly, Wheelchair cushions for persons with spinal cord injury: an update, *Am. J. Occup. Ther.* 45 (6) (1991) 550–554.
- [46] W. Carrigan, P. Nuthi, C. Pande, M.B.J. Wijesundara, C.S. Chung, G.G. Grindle, J.D. Brown, B. Gebrosky, R.A. Cooper, Design and operation verification of an automated pressure mapping and modulating seat cushion for pressure ulcer prevention, *Med. Eng. Phys.* 69 (2019) 17–27.
- [47] A. Sarvazyan, T.J. Hall, M.W. Urban, M. Fatemi, S.R. Aglyamov, B.S. Garra, An overview of elastography-an emerging branch of medical imaging, *Curr. Med. Imag. Rev.* 7 (4) (2011) 255–282.